Differential upper ocean response depicted in moored buoy observations during the pre-monsoon cyclone *Viyaru*

R. Venkatesan, K. Jossia Joseph*, C. Anoopa Prasad, M. Arul Muthiah, S. Ramasundaram and P. Murugesh

National Institute of Ocean Technology, Ministry of Earth Sciences, Chennai 600 100, India

The pre-monsoon cyclone *Viyaru* in the Bay of Bengal during May 2013 traversed a long track from 5°N to 22°N over 7 days with basin-wide response, which was well captured by the time series observations of OMNI buoy network along with satellite data. The differential upper ocean characteristics and its variable response reveal that vertical mixing override horizontal advection during cyclone passage. This study provides insight into the variability in wave spectra, differential response on either side of the track and presence of cold core eddy combined with a thick barrier layer in modulating the upper ocean response.

Keywords: Bay of Bengal, barrier layer, cyclone *Viyaru*, eddies, OMNI buoys, wave spectra.

Introduction

TROPICAL cyclones are one of the major natural hazards accompanied by strong winds, torrential rains and storm surge leading to loss of life and properties which accounts to multi-billion dollars worldwide. The Bay of Bengal, the semi-enclosed basin in North Indian Ocean, experiences less than 6% of global cyclones[1,2] but tops the list in terms of socio-economic impact due to the densely populated low-lying coastal areas. The better prediction of cyclone demands detailed information of the upper ocean dynamics, which was largely missing until the inception of moored buoy network in North Indian Ocean[3,4].

The Bay of Bengal (BoB) experiences intense tropical cyclones during the pre-monsoon (April–May) and the post-monsoon months (October–November), with considerable inter-annual variability in the intensities[5–8]. During pre-monsoon period the Bay is pre-conditioned by warm sea-surface temperature (SST) (>30°C) and low sea-surface salinity (SSS) (<33 psu) which is an important element to support such huge system with enhanced heat transfer from the ocean surface[5]. SST drops by 2–3°C and mixed layer depth (MLD) deepens up to 80 m due to comparatively low salinity stratification in the western and southern BoB[9–11] during pre-monsoon season. During post-monsoon seasons, along the northern and western BoB, SST cooling (~0.3°C) is lower due to intensive salinity stratification and temperature inversion in the upper ocean[12]. Most of the studies that report BoB cyclones are focused on post-monsoon cyclones[8,13–17] and comparatively few studies reported the variability during pre-monsoon cyclones such as *Mala*[8], *Nargis*[5,7] and *Roanu*[18], despite higher response during pre-monsoon cyclones.

The tropical cyclone (TC) *Viyaru* was a pre-monsoon cyclone which formed over the southern BoB near 5°N basin in May 2013 (Figure 1). It formed as a depression, later strengthened into a cyclonic storm (CS) but did not intensify further and maintained a unique quasi-uniform intensity during its life span[19] covering a total distance of about 2150 km in the open ocean. *Viyaru* made its landfall on 16 May 2013 near Chittagong, Bangladesh[20]. The TC *Viyaru* with a long track (https://www.metoc.navy.mil/jtwc) covering south to north in the BoB with a basin-wide response presents perfect plot to analyse the role of pre-monsoon cyclones in the upper ocean dynamics.

Data and methods

Moored buoy data

The primary source of data for the present study is the time series observations from five moored data buoys in the BoB (Figure 1). The moored data buoys are fitted with sensors to measure meteorological and oceanographic parameters such as sea level pressure, air temperature, relative humidity, downwelling long wave and shortwave radiation, wind speed and direction, precipitation, directional wave parameters, temperature and salinity at discrete levels up to 500 m and current profile up to 150 m water depth. The met-ocean parameters are transmitted real-time to the National Institute of Ocean Technology (NIOT), MoES at every three hours and the high frequency data sets are retrieved while servicing the buoy system. The detailed sampling rate, sampling period, resolution, accuracy, range of the sensors are described in Venkatesan *et al.*[4].

*For correspondence. (e-mail: jossiaj@niot.res.in)

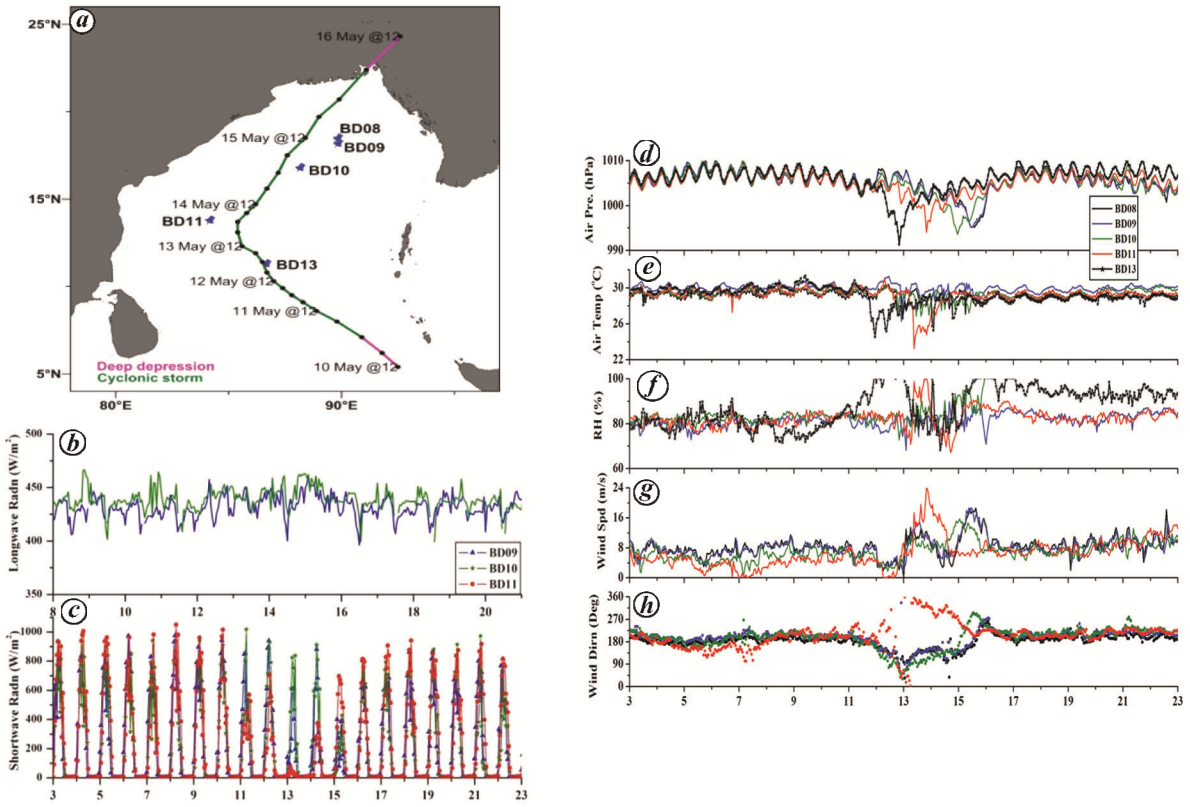

Figure 1. (***a***) Cyclone track of *Viyaru* along with moored buoy network in the Bay of Bengal, surface meteorological observations of moored buoys during cyclone *Viyaru*, (***b***) downwelling long wave radiation, (***c***) downwelling short wave radiation, (***d***) air pressure, (***e***) air temperature, (***f***) relative humidity, (***g***) wind speed and (***h***) wind direction at hourly interval during 3–23 May 2013.

The meteorological and subsurface parameters measured by the OMNI buoy network in BoB at BD08 (18.2°N, 89.67°E), BD09 (17.9°N, 89.68°E), BD10 (16.5°N, 88.0°E), BD11 (13.5°N, 84.0°E) and BD13 (11°N, 86.5°E) are utilized in this study. The buoy BD11 was on the left side of the cyclone track, whereas the remaining buoys were on the right side of the track.

Tropical cyclone heat potential (TCHP) is the oceanic thermal energy available for cyclones, which is a measure of ocean heat content from the surface to the depth of the 26°C isotherm (D26). D26 and TCHP are computed utilizing temperature profiles using the expression[21]

$$\mathrm{TCHP} = \rho C_p \int_0^{D_{26}} [T(z) - 26] \mathrm{d}z,$$

where ρ is the density of sea water at the surface (assumed constant), C_p the specific heat capacity of sea water at constant pressure p, T the temperature (°C) of each layer of ocean thickness dz and D_{26} is the depth of the 26°C isotherm.

In this study, the isothermal layer depth (ILD) was calculated based on temperature difference of 0.5°C. The MLD was estimated based on density variation (σ_t) using the equation of state[22]

$$\Delta\sigma_t = \sigma_t(T - \Delta T, S, P) - \sigma_t(T, S, P),$$

where $\Delta\sigma_t$ is the computed density difference criterion, $\sigma_t(T, S, P)$ is the density computed based on temperature and salinity at the surface, and $\sigma_t(T - \Delta T, S, P)$ is the density computed equivalent to a temperature difference of 0.5°C from the surface. ILD and MLD were calculated relative to the 10 m depth. The difference between the three-day averaged temperature and salinity profiles before and after the cyclone passage is used to identify the immediate response in thermohaline structure.

Satellite data

In addition to *in situ* measurements from moored buoy network, satellite products of SST, SSS, wind and sea level anomaly (SLA) are utilized to envisage the spatial response. In order to understand the general circulation pattern in BoB, the Ocean Surface Current Analysis Real-time (OSCAR) surface zonal and meridional velocity is utilized[23]. The data is available on global 1/3° grid with 5-day temporal resolution (http://www.esr.org/oscar_index.html). The atmospheric response is analysed from the daily zonal and meridional wind speed from Advanced Scatterometer (ASCAT) having a spatial

resolution of $0.25° \times 0.25°$ (http://apdrc.soest.hawaii.edu). SST during cyclone period is obtained from daily Group for High Resolution Sea Surface Temperature (GHRSST) ($0.01° \times 0.01°$), (https://podaac.jpl.nasa.gov/GHRSST). The SSS data from Aquarius sensor onboard the SAC-D satellite, available at 1° spatial resolution and weekly temporal scale (http://apdrc.soest.hawaii.edu) is utilized to understand the salinity variability.

Observations

The advancement in satellite technology enabled the tracking and forecast of the basin-wide response of *Viyaru* from its genesis to landfall, especially in data-sparse regions of BoB. The high frequency subsurface moored buoy observations along with synoptic remote-sensing observations provide a comprehensive view of upper ocean response. The observations are classified as pre- (3–9 May 2013), during (10–16 May 2013) and post- (17–23 May 2013) cyclone period to infer the response in upper ocean dynamics.

Spatial response observed in satellite measurements

The wind speed, SST, SSS and SLA overlaid with surface current presented in Figure 2 demonstrate the spatial response of *Viyaru* in BoB. The weekly averaged wind showed prevalence of predominantly southerly and southeasterly winds in BoB before and after the cyclone passage (Figure 2 *a*). Strong cyclonic winds close to the track and southwesterly winds close to the coastal areas were observed during the cyclone passage.

The GHRSST showed higher SST (more than 30°C) in the central BoB and lower SST in the northern bay before the cyclone passage. It is evident that *Viyaru* intensified into cyclone after coming across warm waters in the central BoB (Figure 2 *b*). Significant reduction in SST (29°C) was observed along the cyclone track, particularly in central bay after cyclone passage. The cooling at the northern bay was rapid, whereas the cooling at central bay was gradual. The significant spatial gradient in SST before the cyclone passage is brought down to near uniform SST in entire BoB except in coastal regions, indicating basin-wide response of *Viyaru*.

The SSS (Figure 2 *c*) was comparatively low in the northeastern bay before the cyclone, which increased close to the track during cyclone passage. Patches of less saline water were observed after the cyclone passage in northeastern bay. The mesoscale eddies as evident from surface current (Figure 2 *d*) could have significantly influenced the upper ocean response, particularly the pathways of less saline water. A slight weakening of the cyclonic eddy centred around BD10 as well as nearby warm core eddies is observed after the cyclone passage. The salinity distribution in BoB is favoured by the advection of eddies as revealed by the pulsating signals in SSS with a lag at BD11, BD09 and BD08 locations.

Surface meteorological observations

All moored buoys in BoB captured the signals of *Viyaru* with earliest response at BD13 (11°N, 86.5°E) on 11 May, which continued till BD08 at ~18.2°N on 15 May indicating basin-wide response. The buoy BD13 was closest to the track and exhibited maximum response, whereas BD11 on left side of the track showed the minimal response due to relative position.

The diurnal variability observed in air pressure, air temperature and radiation measurements was significantly reduced in response to cyclone passage along with considerable changes in wind speed and directions (Figure 1).

The downwelling longwave radiation displayed reduction in diurnal variability and slightly higher values during the cyclone passage (Figure 1 *b*). The downwelling shortwave radiation was more than 900 W/m^2 at all buoy locations before 10 May. The low pressure system with intense cloud cover inhibits the downwelling shortwave radiation to less than 75 W/m^2 at BD11 on 13 May and less than 500 W/m^2 at BD09 and BD10 on 15 May (Figure 1 *c*).

The minimum air pressure of 991.36 hPa was recorded at BD13 on 12 May followed by 993.59 hPa at BD10 on 14 May (Figure 1 *d*). A sudden drop in air temperature associated with the passage of cyclone is observed at BD11 and BD13 recording a minimum of 23.2°C and 24.5°C, accounting for a drop of ~6°C and ~5.5°C respectively, with considerable reduction in diurnal oscillation (Figure 1 *e*). The relative humidity in the entire BoB remained high (~80%) which showed sudden peak during passage of *Viyaru* (Figure 1 *f*).

The sudden increase in wind speed is observed at all buoy locations, which reached a maximum of 21.1 m/s at BD11 (Figure 1 *g*). The wind direction during pre- and post-cyclone passage was predominantly southerly, which exhibited near clockwise circulations except at BD11, which exhibited an anticlockwise rotation owing to the relative position of the moored buoy (Figure 1 *h*). The impact at BD13 remained for a longer period leading to stronger inertial currents and higher response in mixed layer.

Response in sea state

The wave parameters exhibited sudden change in sea state associated with the *Viyaru* (Figure 3). In general, the sea state was calm before cyclone passage with significant wave height less than 2 m. The mean wave direction exhibited steady southerly waves at central bay whereas

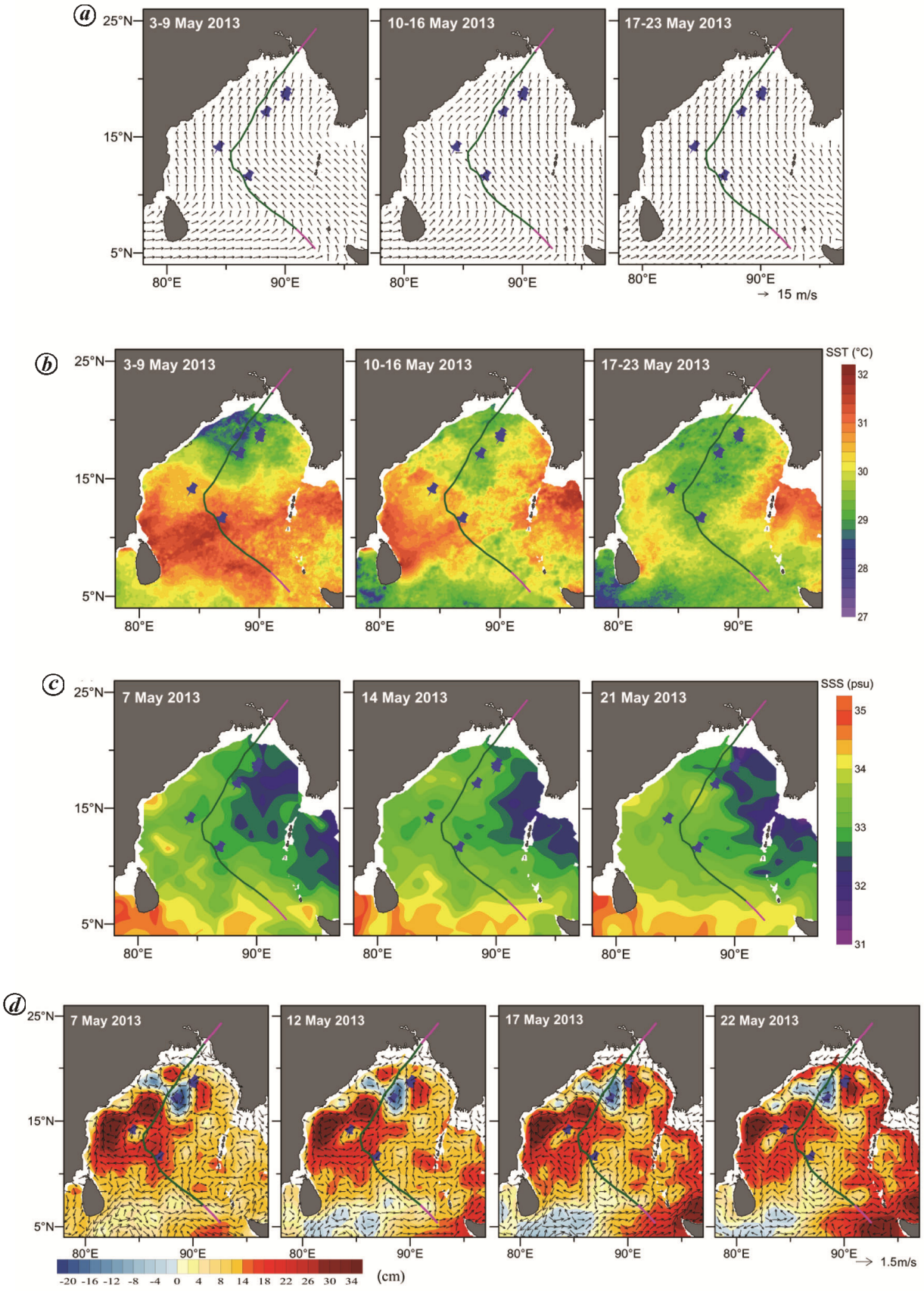

Figure 2. The spatial observations of (***a***) wind speed, (***b***) sea-surface temperature, (***c***) sea-surface salinity and (***d***) sea level anamoly overlaid with surface currents before, during and after the cyclone passage.

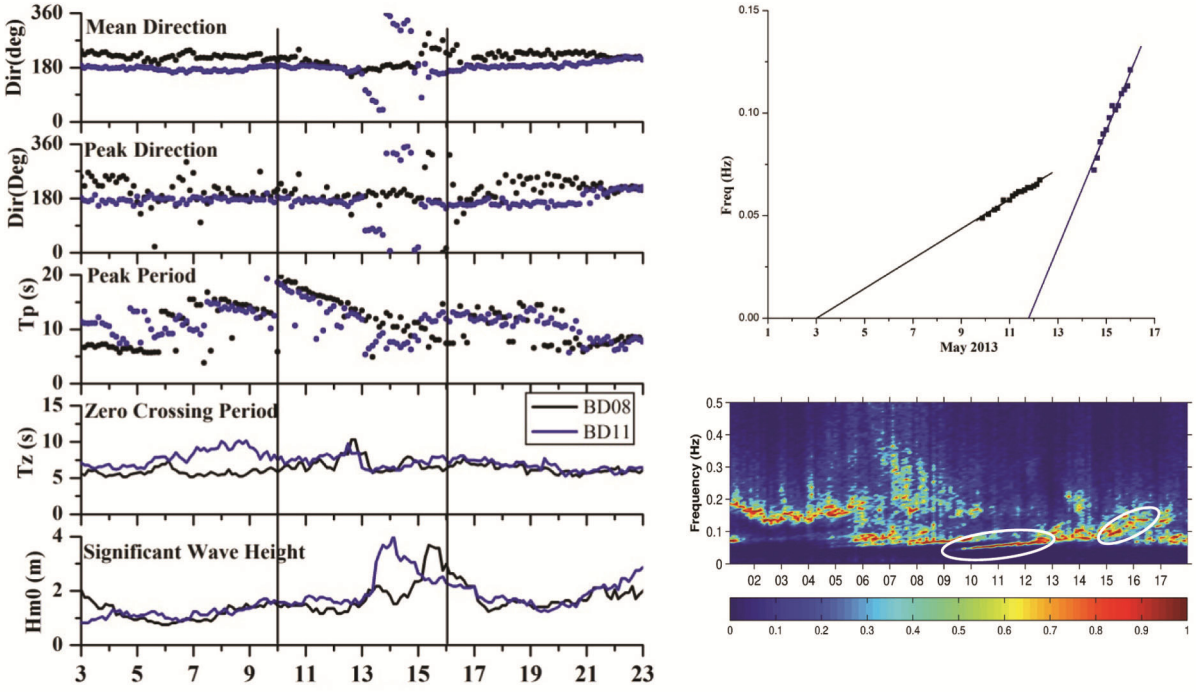

Figure 3. Time series observations of hourly wave parameters before, during and after the passage of the cyclone *Viyaru* at central bay and at northern bay (left panel) during 3–23 May 2013, the ridge analysis of peak period at northern bay (right top) and the wave spectra (m^2/Hz) indicating the arrival of long swells at northern bay (right bottom).

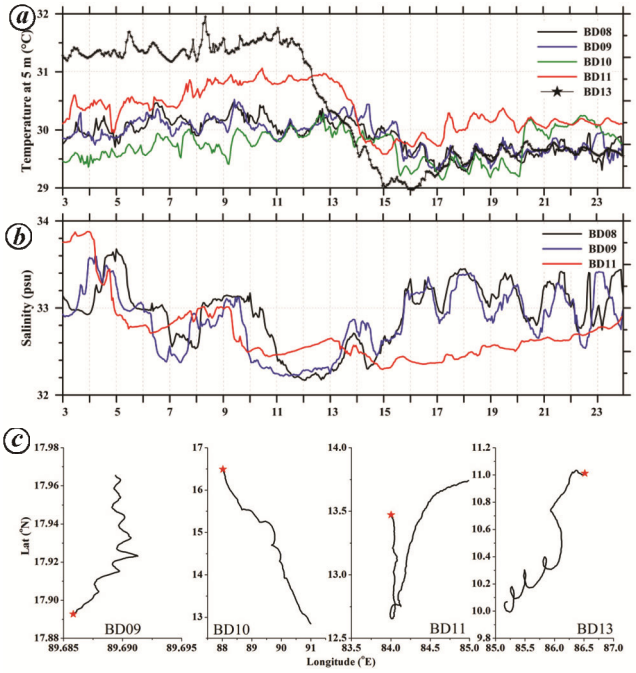

Figure 4. (***a***) Sea-surface temperature (5 m depth); (***b***) sea-surface salinity (5 m depth except 1 m depth at BD09) and (***c***) progressive vector diagram during 3–23 May 2013.

at the northern bay waves were steady southwesterly. The maximum significant wave height observed at central bay was 4 m (14 May) whereas that at northern bay was 3.7 m (15 May).

The detailed analysis of peak period indicates the presence of swells during the first half of May (Figure 3). It revealed the arrival of long swell train at 21 GMT on 9 May, followed by short swells on 14 May at northern bay. The dispersive arrival of swells with highest period followed by shorter period exhibits a ridge line, which points to the origin as well as speed of the swells. The analysis revealed that the long swells might have originated on early hours on 3 May which coincided with the Severe Tropical Cyclone Zone off Australia in southwest Pacific Ocean during 27 April to 3 May. The short swells indicated the origin on 11 May and are the forerunners of the cyclone *Viyaru*. The long swells took more than six days to reach the buoy location at northern bay whereas the forerunners reached within 42 h. The presence of the long swells along with the forerunners and sea waves generated by *Viyaru* aggravated the rough sea state in northern BoB.

Upper ocean response

The immediate response to *Viyaru* was observed in the substantial lowering of the SST (Figure 4 *a*). The northern bay (18°N) exhibited SST around 30°C, whereas the minimum SST was observed at BD10 location (16.5°N). The maximum SST (more than 31.5°C) was at southern location (BD13), followed by BD11 at west-central bay (>30.5°C). Maximum drop in SST (2.5°C) was observed

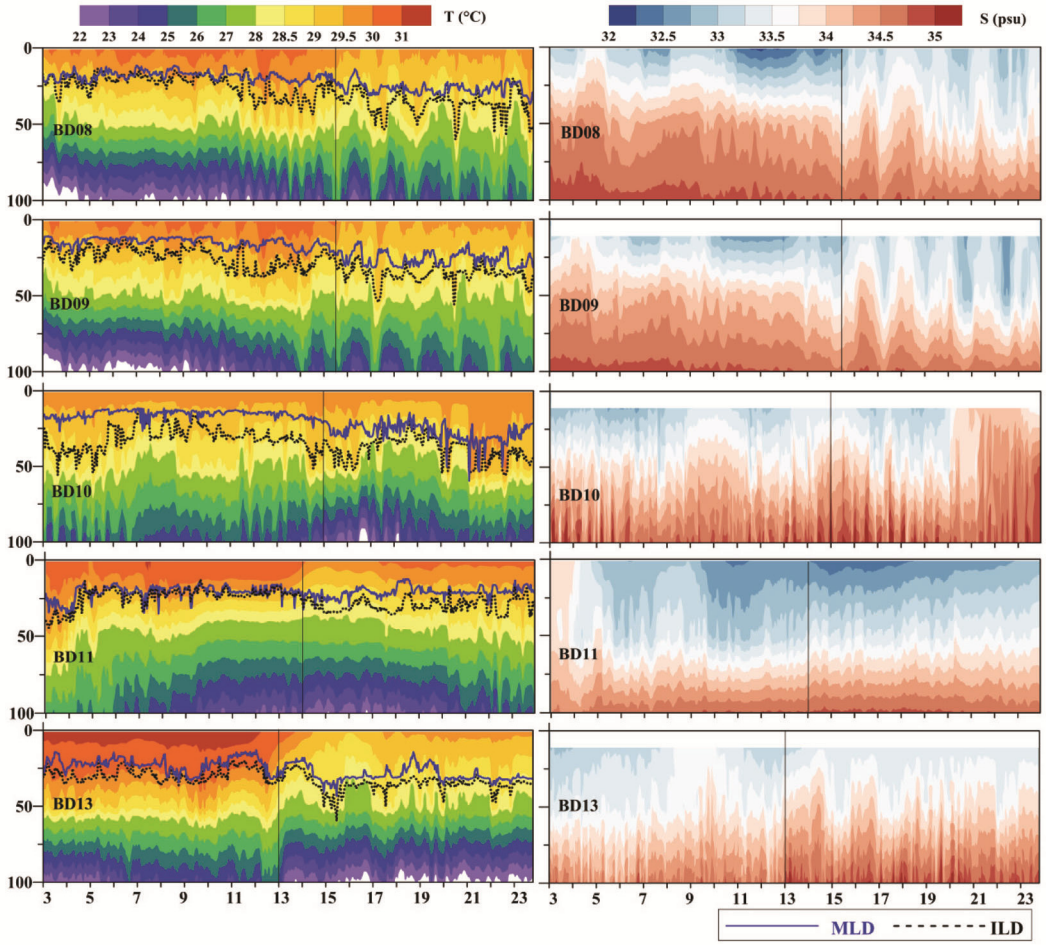

Figure 5. The hourly time series observations of temperature (left panel) overlaid with isothermal layer depth (dotted black line) and mixed layer depth (blue line) and salinity (right panel) during 3–23 May 2013. Black vertical line indicates the cyclone passage at the buoy location.

at BD13, which dropped from more than 31.5°C on 11 May to 29°C on 14 May, followed by 1.5°C drop at BD11 location and 1°C drop at the remaining locations. An interesting observation is the nearly uniform post-cyclone SST on the right side of the track indicating wide spread cooling whereas that of BD11 remained warmer due to the asymmetric cooling on the left side of the cyclone track (Figure 4 *a*).

The SSS at BD08, BD09 and BD11 reveals the presence of a pulsating signal of nearly the same amplitude with a periodicity of ~5 days before cyclone passage (Figure 4 *b*). The SSS was more than 33.5 psu during pre-cyclone period, which reduced by 1 psu at all locations. The salinity at BD08 and BD09 locations exhibited oscillations at inertial period after the passage of cyclone, whereas the BD11 remained comparatively less saline.

The surface current indicates variability induced by the relative position of the buoys (Figure 4 *c*), which demonstrates northward flow at BD09, southwestward flow at BD13 and southeastward flow at BD10. These buoys were on right side of the track and regained the nearly pre-cyclonic net current direction after the cyclone passage. On the other hand, BD11 buoy which was on the left side of the track changed its pre-cyclonic southward direction to northeastward after cyclone passage. The OSCAR data (Figure 2 *d*) reveals the presence of eddies close to the buoy locations and also supports the variability observed in current direction.

The surface current speed at BD10 before cyclone passage was ~50 cm/s, which reached a maximum of 140 cm/s on 15 May (Figure 4 *c*). Significant semidiurnal oscillation with a magnitude of ~20 cm/s was observed at BD13. The intense momentum transferred to the mixed layer during the cyclone passage was reflected as significant increase in surface current speed, which also triggered inertial oscillations on the right side of the track[24] as indicated in the progressive vector diagram (Figure 4 *c*). The inertial currents particularly at BD13, which remained for a longer period, could have contributed for the significant drop in temperature.

The temperature profile depicts typical pre-cyclone temperature profile (Figure 5) at BD08, BD09, BD11 and BD13 exhibited pre-monsoon conditions in the BoB with 20–30 m MLD and warmer SST (>30°C). The deeper

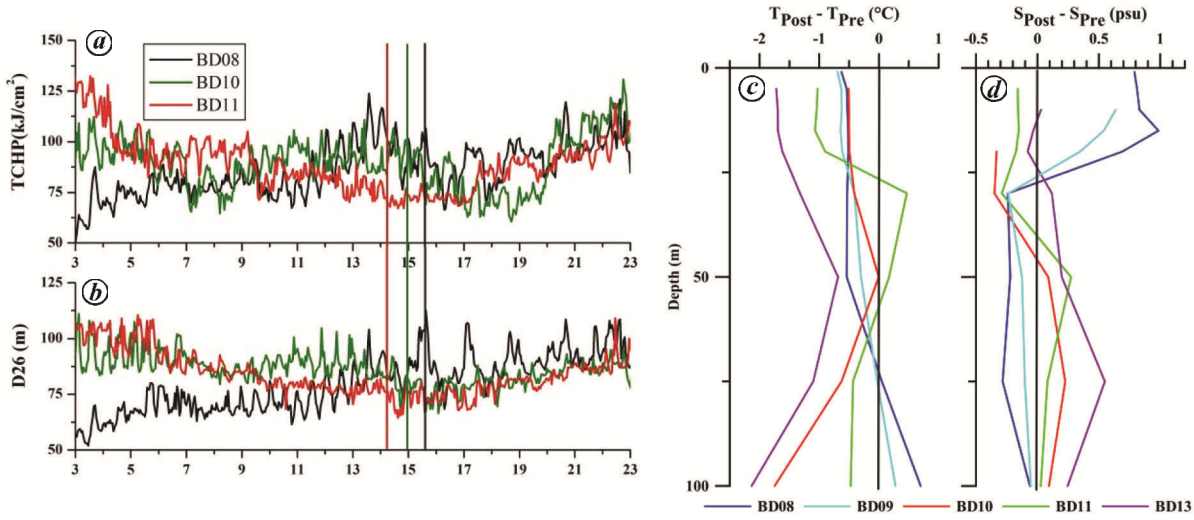

Figure 6. (***a***) Tropical cyclone heat potential, (***b***) depth of 26°C isotherm at BD08, BD10 and BD11 during 3–23 May 2013, (***c***) three-day averaged temperature difference (T_{Post}–T_{Pre}) and (***d***) three-day averaged salinity difference (S_{Post}–S_{Pre}) between post-cyclone and pre-cyclone period.

layers showed significant semidiurnal oscillation at all locations. Shallow MLD with barrier layer of ~20 m was observed at BD10 with an anomalously low SST due to the presence of cold core eddy evident from SLA (Figure 2 *d*). It was interesting to note that the cyclone induced wind forcing could break the barrier layer but the presence of deeper ILD reduced the cooling in MLD. Less saline surface water was observed at northern bay (BD08 and BD09) and at BD11 similar pulsating signals in salinity profile (Figure 5) was observed as in SSS. The wind induced mixing resulted in increasing the mixed layer salinity except at BD11, which exhibited significant freshening. Significant oscillations in near inertial period were observed in temperature and salinity profiles at BD08, BD09 and BD13 after the cyclone, which enhanced the cooling supported by the shoaling of isotherms[13]. BD11 on the left side of the track and BD10 at the centre of the cold core eddy did not exhibit any significant inertial currents in temperature and salinity profiles, but the semidiurnal oscillations continued.

The difference between the three-day averaged temperature and salinity profiles before and after the cyclone passage indicated significant cooling at the surface with a subsurface minimum in the upper thermocline depth except at northern bay (Figure 6 *c*). BD11 on the left side of the track indicated subsurface warming followed by cooling at deeper layers. Minimum cooling of mixed layer observed at BD10 was attributed to the combined effect of barrier layer[12] and cold core eddy. The warming at subsurface layers of BD08 and BD09 was favoured by the displacement of isotherms forced by inertial oscillation. The salinity increased significantly in surface layers of BD08 and BD09, followed by minimal increase in subsurface layers. The remaining buoys showed similar salinity response with increase in surface layers and decrease in subsurface layers.

The TCHP (Figure 6 *a*) and D26 (Figure 6 *b*) demonstrated significant spatial variability before *Viyaru*. At BD11, TCHP higher than 125 kJ/cm^2 reduced gradually during cyclone (<75 kJ/cm^2) and BD10 also exhibited decreasing trend. The BD08 with minimum TCHP (~50.1 kJ/cm^2) showed an increasing trend which peaked (124.8 kJ/cm^2) just before the cyclone passage and reduced to lesser than 75 kJ/cm^2 after the cyclone. All three locations exhibited deepening of D26 immediately after the cyclone passage (Figure 6 *b*).

Conclusions

The moored buoy observations reveal variable response to cyclones triggered by the proximity, relative location, presence of barrier layer and a cold core eddy. The asymmetric response is well depicted by the lesser cooling and lack of inertial oscillation on left side of the track. The deep ocean wave spectra reveal the arrival of swells from southern ocean and forerunners of cyclone *Viyaru* at northern bay. The presence of cold core eddy along with thick barrier layer in the west-central BoB restricted the upper ocean response particularly the reduction in mixed layer cooling.

1. Alam, Md. M., Hossain, Md. A. and Shafee, S., Frequency of Bay of Bengal cyclonic storms and depressions crossing different coastal zones. *Int. J. Climatol.*, 2003, **23**, 1119–1125.
2. Akter, N. and Tsuboki, K., Role of synoptic-scale forcing in cyclogenesis over the Bay of Bengal. *Clim. Dyn.*, 2014, **43**, 2651–2662.
3. Premkumar, K., Ravichandran, M., Kalsi, S., Sengupta, D. and Gadgil, S., First results from a new observational system over the Indian Seas. *Curr. Sci.*, 2000, **78**(03), 323–330.

4. Venkatesan, R. *et al.*, *In situ* ocean subsurface time-series measurements from OMNI buoy network in the Bay of Bengal. *Curr. Sci.*, 2013, **104**, 1166–1177.
5. Maneesha, K., Murty, V. S. N., Ravichandran, M., Lee, T., Yu, W. and McPhaden, M. J., Upper ocean variability in the Bay of Bengal during the tropical cyclones *Nargis* and *Laila*. *Prog. Oceanogr.*, 2012, **106**, 49–61.
6. Obasi, G. O. P., WMO's programme on tropical cyclone. *Mausam*, 1997, **48**, 103–112.
7. McPhaden, M. J. *et al.*, Ocean–atmosphere interactions during cyclone *Nargis*. *EOS Trans. Am. Geophys. Union*, 2009, **90**, 53–54.
8. Vissa, N. K., Satyanarayana, A. N. V. and Prasad Kumar, B., Response of upper ocean during passage of MALA cyclone utilizing ARGO data. *Int. J. Appl. Earth Obs. Geoinf.*, 2012, **14**, 149–159.
9. Gopalakrishna, V. V., Murty, V. S. N., Sarma, M. S. S. and Sastry, J. S., Thermal response of upper layers of Bay of Bengal to forcing of a severe cyclonic storm: a case study. *Indian J. Geo-Mar. Sci.*, 1993, **22**, 8–11.
10. Behera, S. K., Deo, A. A. and Salvekar, P. S., Investigation of mixed layer response to Bay of Bengal cyclone using a simple ocean model. *Meteorol. Atmosph. Phys.*, 1998, **65**, 77–91.
11. Neetu, S. *et al.*, Influence of upper-ocean stratification on tropical cyclone-induced surface cooling in the Bay of Bengal. *J. Geophys. Res. Oceans*, 2012, **117**(C12), C12020.
12. Sengupta, D., Goddalehundi, B. R. and Anitha, D. S., Cyclone-induced mixing does not cool SST in the post-monsoon north Bay of Bengal. *Atmosph. Sci. Lett.*, 2008, **9**, 1–6.
13. Girishkumar, M. S. *et al*., Observed oceanic response to tropical cyclone *Jal* from a moored buoy in the south-western Bay of Bengal. *Ocean Dyn.*, 2014, **64**, 325–335.
14. Joseph, K. J., Balchand, A. N., Hareeshkumar, P. V. and Rajesh, G., Inertial oscillation forced by the September 1997 cyclone in the Bay of Bengal. *Curr. Sci.*, 2007, **92**, 790–794.
15. Vissa, N. K., Satyanarayana, A. N. V. and Kumar, B. P., Response of upper ocean and impact of barrier layer on Sidr cyclone induced sea surface cooling. *Ocean Sci. J.*, 2013, **48**, 279–288.
16. Navaneeth, K. N., Martin, M. V., Joseph, K. J. and Venkatesan, R., Contrasting the upper ocean response to two intense cyclones in the Bay of Bengal. *Deep Sea Res. Part Oceanogr. Res. Pap.*, 2019, **147**, 65–78.
17. Mathew, S., Natesan, U., Latha, G., Venkatesan, R., Rao, R. and Ravichandran, M., Observed warming of sea surface temperature in response to tropical cyclone *Thane* in the Bay of Bengal. *Curr. Sci.*, 2018, **114**, 1407–1413.
18. Mandal, S., Sil, S., Shee, A. and Venkatesan, R., Upper ocean and subsurface variability in the Bay of Bengal during cyclone *Roanu*: a synergistic view using *in situ* and satellite observations. *Pure Appl. Geophys.*, 2018, **175**, 4605–4624.
19. Kotal, S. D., Bhattacharya, S. K., Bhowmik, S. K. R. and Kundu, P. K., Growth of cyclone *Viyaru* and *Phailin* – a comparative study. *J. Earth Syst. Sci.*, 2014, **123**, 1619–1635.
20. A preliminary report on cyclonic storm, *Viyaru* over Bay of Bengal (10–16 May 2013), IMD, 2013.
21. Leipper, D. F. and Volgenau, D., Hurricane heat potential of the Gulf of Mexico. *J. Phys. Oceanogr.*, 1972, **2**, 218–224.
22. Kara, A. B., Rochford, P. A. and Hurlburt, H. E., An optimal definition for ocean mixed layer depth. *J. Geophys. Res. Oceans*, 2000, **105**, 16803–16821.
23. Bonjean, F. and Lagerloef, G. S. E., Diagnostic model and analysis of the surface currents in the tropical Pacific Ocean. *J. Phys. Oceanogr.*, 2002, **32**, 2938–2954.
24. Price, J. F., Upper ocean response to a hurricane. *J. Phys. Oceanogr.*, 1981, **11**, 153–175.

ACKNOWLEDGEMENTS. We thank the Director of NIOT, Chennai and the Ministry of Earth System Sciences, Govt of India, for the support and encouragement. We also thank the staffs of Ocean Observation Systems, NIOT for the maintenance of moored buoy network.

doi: 10.18520/cs/v118/i11/1760-1767